2019 IEEE Intelligent Transportation Systems Conference (ITSC)
Auckland, NZ, October 27-30, 2019

Range-based Cooperative Localization with Nonlinear Observability Analysis

Brandon Araki[1], Igor Gilitschenski[1], Tatum Ogata[1], Alex Wallar[1],
Wilko Schwarting[1], Zareen Choudhury[1], Sertac Karaman[2], and Daniela Rus[1]

***Abstract*— Accurate localization of other cars in scenarios such as intersection navigation, intention-aware planning, and guardian systems is a critical component of safety. Multi-robot cooperative localization (CL) provides a method to estimate the joint state of a network of cars by exchanging information between communicating agents. However, there are many challenges to implementing CL algorithms on physical systems, including network delays, unmodeled dynamics, and non-constant velocities. In this work, we present a novel experimental framework for range-based cooperative localization that enables the testing of CL algorithms in realistic conditions, and we perform experiments using up to five cars. For state estimation, we develop and compare a particle filter, an Unscented Kalman Filter, and an Extended Kalman Filter that are compatible with nonlinear dynamics and the asynchronous reception of messages. We also model the relative transform between two unicycle models and perform a nonlinear observability analysis on the system, giving us insight into the measurements required to estimate the system's state. Our approach enables relative localization of multiple vehicles in the absence of any global reference frame or joint map, and we demonstrate the effectiveness of our system in real-world experiments. Our results show that the UKF is likely the best candidate to use for the CL task.**

I. Introduction

Situational awareness in traffic is a key functionality of autonomous driving [1]. In particular, accurate localization of other cars is especially important for intention-awareness in maneuvers such as merging and unprotected left-hand turns. In these scenarios perceiving even a small change in velocity or bearing by the other cars can impact decision making and the safety of the current maneuver. In order to obtain the location of relevant surrounding vehicles, it is not sufficient to rely on a car's typical sensors, which usually consist of a combination of LiDARs, radars, and cameras. These sensors do not receive direct state measurements of the other cars but instead must estimate their states indirectly; furthermore, they are not capable of perceiving other cars that are not in line of sight.

Recent developments in Vehicle-to-Vehicle (V2V) communication systems support alternative solutions to localization [2], [3], [4]. A car can obtain its position when it is localized against a previously created map or when information from a Global Navigation Satelite System (GNSS) such as the Global Positioning System (GPS) is available.

[1]Massachusetts Institute for Technology, Computer Science and Artificial Intelligence Lab (CSAIL), Cambridge, MA, USA.
[2]Massachusetts Institute for Technology, Laboratory for Information and Decision Systems (LIDS), Cambridge, MA, USA.
Contact: araki@mit.edu

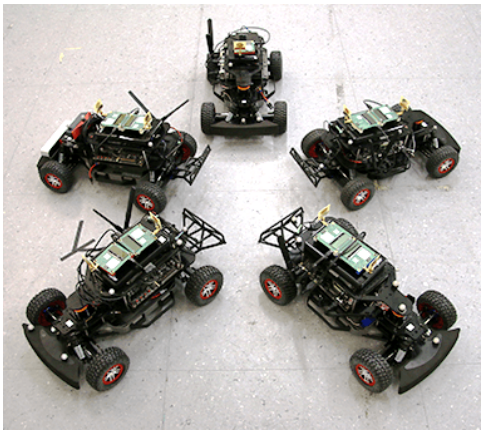

Fig. 1: The range-based cooperative localization system proposed in this work is deployed and evaluated on five MIT Racecar [5] platforms with a sensor setup similar to the setup on autonomous cars.

This position can be sent out to the other vehicles in its environment using V2V communication. In practice, it is not feasible to rely on permanent availability of an up-to-date map or on the availability of a GPS signal. The former can happen when environmental changes make localization in existing maps unreliable or in mapless driving applications which do not assume the existence of a map. Loss of GPS signal can occur in tunnels and in urban driving scenarios where buildings hinder satellite connectivity.

In the absence of global positioning data, a distributed cooperative localization scheme in which cars perform relative position measurements and exchange their odometry information using V2V communication could provide a better solution. In this work, we consider the cooperative localization problem assuming that the cars are capable of exchanging relative range measurements. While it has been shown that it is more challenging to localize with relative range measurements than with relative bearing measurements [6], relative bearing measurements are harder to obtain, since implementations rely on visual tracking to estimate bearing and therefore require full visibility of the other cars [7], [8]. Ultra-wideband (UWB) radio systems, by contrast, can provide accurate range measurements even in non-line-of-sight scenarios by taking into account multi-path effects. While numerous approaches have considered cooperative localization scenarios, they typically assume the existence of a global reference frame, rely on additional

978-1-5386-7024-8/19/$31.00 ©2019 IEEE

bearing measurements, or do not consider the underlying system dynamics [9], [10], [11].

In our work, we propose a new system that estimates the relative positions of surrounding vehicles from UWB range measurements and odometry information. UWB range measurements are reliable to within 10 cm at ranges of up to 100 m [12], which covers most intersections in complex road networks. Our solution requires no outside infrastructure and is distributed, so that each vehicle shares its range measurements with cars in its network. Using a particle filter, Unscented Kalman Filter (UKF), or Extended Kalman Filter (EKF), the car estimates the locations of the other cars in its neighborhood, whether they are in line-of-sight or not. We also discuss the architecture of the cooperative localization system and explain the individual design choices. The system is evaluated in physical experiments using up to five cars. Overall, this paper contributes the following:

1) A comparison of a particle filter, UKF, and EKF for cooperative relative localization of multiple vehicles using just odometry and UWB range measurements.
2) A model of the relative transform between two unicycle models and the corresponding nonlinear observability analysis.
3) An experimental multi-robot platform for cooperative localization.
4) Evaluation in physical experiments with up to five vehicles in which the assumptions made in other works are relaxed, i.e., time delays and packet loss on the network; varying linear and angular velocities while driving; asynchronous reception of range and odometry measurements; no stationary landmarks/beacons; and no measurements in a global coordinate system.

II. Related Work

The multi-robot cooperative localization (CL) problem, in which the state of the system is estimated through some form of information exchange between the nodes of a network, has been approached from many different angles. In map-based multi-robot localization, multiple agents collaborate in order to create or localize from a joint map. Multi-robot map creation can be carried out in an offline fashion where multiple maps are, topologically or metrically, co-registered to each other [13], [14]. Recent work has also investigated scenarios where several agents simultaneously create a joint map [15], [16], [17]. Although these approaches can be very accurate and also result in the construction of a shared map of the environment, their downside is that they require significant data collection and exchange and also impose a significant burden on computational power and data transfers in order to create and synchronize a given map online. Our approach operates in a purely mapless fashion and thus requires neither the existence of a joint map nor potentially costly synchronization mechanisms.

There has also been a considerable amount of research focusing on cooperative localization without assuming the use of a map. These approaches often focus on estimating the relative transforms between agents using a combination of proprioceptive measurements, such as odometry, and exteroceptive measurements, most commonly relative range, bearing, and orientation measurements. EKFs are often used to estimate the state of the system [18], [19], [20]; their advantages are that they are computationally efficient and easy to analyze, resulting in bounds on error and covariance estimates such as in [9], [10]. If both relative range and bearing measurements are available, they can be converted into an estimate in Cartesian coordinates and easily linearized. Other approaches tackle the issue of nonlinearity by using a particle filter, UKF, or other more specialized filters such as the Cubature Kalman Filter to estimate the posterior likelihood density; they also often incorporate consensus schemes to share estimates across a network [21], [22], [23], [24], [11], [25]. However, the exchange of states rather than the raw measurements may introduce common process noise into the estimate and requires special treatment, e.g. by using methods such as covariance intersection [26]. We compare the performance of a particle filter, UKF, and EKF on our nonlinear model and exchange range and odometry measurements between cars.

Although the analysis of nonlinear models is much more difficult than in the case of a linearized system, nonlinear observability analyses have been performed on cooperative localization systems. [27] performs a nonlinear observability analysis on a single unicycle robot that can take range measurments of its environment. [6] performs an observability analysis on a two-robot system using a relative model in polar coordinates, and they compare range, bearing, and orientation measurements, as well as the necessity of odometry measurements. We perform a similar analysis for range measurements in Cartesian coordinates. [28] extends the analysis of the two-car system with only bearing measurements to the N-car case. In [29], an observability analysis is performed for robots in a 3D underwater environment.

While most works consider the theoretical aspects of cooperative localization, there have been several experiments demonstrating a fully integrated real-world system. In [30], [31], a relative transform is estimated in the context of situational awareness and tracking occluded operators from a UAV. In contrast to those works, our work simultaneously estimates relative transforms for a group of vehicles. An application with multiple cars is presented in [8] using bearing measurements, which requires direct visibility to estimate. The work presented in [32] considers relative localization for a group of micro air vehicles based on range measurements using an EKF. Experiments using Autonomous Underwater Vehicles (AUVs) are presented in [33], [34]. In contrast to previous work, our experiments use a driving platform with a unicycle model, and given the nonlinearity of the dynamics and measurement models we evaluate three different filters.

III. System Model

We consider a 2D multirobot system indexed by $\Omega = \{1, \ldots, N\}$. We do not consider the absolute position of the robots but rather the relative transformations between the robots.

The measurement graph between robots is defined by a *relative position measurement graph* (RPMG), adopted from [9]. In our case, this graph defines which pairs of robots can take relative range measurements of the other's position. In this work, we assume that the measurement graph is complete, i.e. every robot ranges with every other robot. We call the set of other robots with which robot i can range the neighbors of robot i, $\mathcal{N}_i$.

Each robot i estimates the transformation between its local frame and its neighbors' local frames, so that the state space is defined as $T_i = \{T_{ji} | i \in \Omega, j \in \mathcal{N}_i\}$. A single transformation is defined as $T_{ji} = [x_{ji}, y_{ji}, \theta_{ji}]^T \in SE(2)$.

A. Motion Model

The inputs are from odometry measurements of linear and angular velocity, $u_i = \{v_i, \omega_i\}$. All robots are assumed to have a unicycle motion model,

$$\frac{dT_{ji}}{dt} = \begin{bmatrix} v_j \cos\theta_{ji} \\ v_j \sin\theta_{ji} \\ \omega_j \end{bmatrix} + \begin{bmatrix} y_{ji}\omega_i - v_i \\ -x_{ji}\omega_i \\ -\omega_i \end{bmatrix}. \tag{1}$$

The first part of Eq. 1 represents the effect of robot j on T_{ji} – this is simply the unicyle model. The second term models the effect of robot i on its own transform. The effect of angular velocity ω_i on the transform, assuming all other inputs are 0, is modeled by $\frac{dT_{ji}}{dt} = -\omega_i \times r$, where $r = [x_{ji}, y_{ji}]^T$. This can be reformulated as a dot product using the angular velocity tensor $W = \begin{bmatrix} 0 & \omega_i \\ -\omega_i & 0 \end{bmatrix}$ as

$$\frac{dT_{ji}}{dt} = W \cdot r = \begin{bmatrix} y_{ji}\omega_i \\ -x_{ji}\omega_i \end{bmatrix}.$$

We assume a continuous-time model and approximate the next state using the Runge-Kutta method.

B. Observation Model

Besides the odometry measurements, which we integrate into the motion model, we take only range measurements from the UWB sensors. We define an observation o_{ji} as robot i's range measurement of robot j,

$$o_{ji} = \sqrt{x_{ji}^2 + y_{ji}^2}. \tag{2}$$

Note that this range measurement is nonlinear and gives no information on the relative angle θ_{ji} between the frames of the robots. Unlike other works that linearize the dynamics and measurement models, we do not assume a bearing measurement, which could be used to linearize the model. Nevertheless, our model is observable, as shown in [6].

C. Nonlinear Observability Analysis

Since we use a nonlinear dynamics model, we cannot analyze the observability of our system using the observability matrix from linear systems. We therefore perform a nonlinear observability analysis on the two-car system. Our analysis is similar to the one performed in [6], but using a different coordinate system. The concept of nonlinear observability is undergirded by the concept of *indistinguishability*, as defined

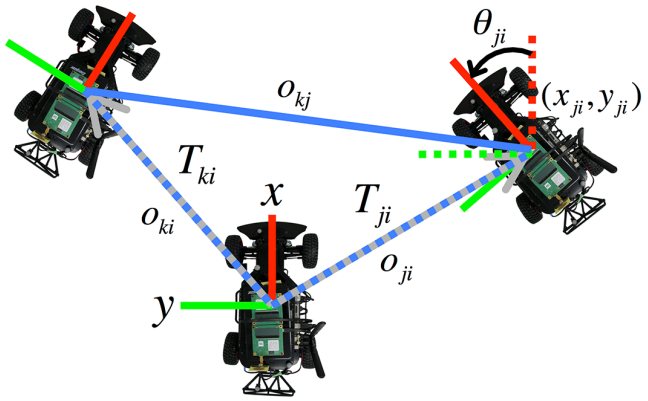

Fig. 2: Grey arrows represent the transforms between ego car i and other cars j and k. Blue lines represent range measurements and the red and green arrows represent the x- and y-axes of each car's local frame.

in [35]. Let $\mathcal{T}$ be the C^∞ *3-dimensional manifold* of our system, and let U be a subset of $\mathcal{T}$. Furthermore, let $x_0, x_1 \in \mathcal{T}$. Then x_0 is *U-indistinguishable* from x_1 if for every control u, the trajectories $x(t_0, t_1, x_0, u)$ and $x(t_0, t_1, x_1, u)$ both lie in U and cannot be used to distinguish between x_0 and x_1. A system is *locally weakly observable at* x_0 if there exists a neighborhood U of x_0 such that if a point $x_1 \in U$ is *U-indistinguishable* from x_0, then $x_0 = x_1$. A system is *locally weakly observable* if this is the case for all $x \in \mathcal{T}$.

Note that our model Eq. 1 is affine in the inputs and can therefore be represented as

$$\dot{T}_{ji} = \sum_{k=1}^{4} g_k(T) u_k, \tag{3}$$

where

$$g_1(T) = [-1, 0, 0]^T \qquad g_2(T) = [y_{ji}, -x_{ji}, -1]^T$$
$$g_3(T) = [\cos\theta_{ji}, \sin\theta_{ji}, 0]^T \qquad g_4(T) = [0, 0, 1]^T.$$

Let $o_{ji} : \mathcal{T} \longrightarrow Y = \mathbb{R}$ be the smooth output map of the system. The *observation space* $\mathcal{O}$ of the system is defined as the linear space of functions on $\mathcal{T}$ containing o_{ji} and all repeated Lie derivatives:

$$\mathcal{O} = \text{span}\, \mathcal{L}_{Z_1} \mathcal{L}_{Z_2} \cdots \mathcal{L}_{Z_k} o_{ji}, \tag{4}$$

with Z_i, $i \in k$, in the set $\{g_1, \ldots, g_4\}$. Note that because $\mathcal{L}_{X_1} + \mathcal{L}_{X_2} H = \mathcal{L}_{X_1} H + \mathcal{L}_{X_2} H$ and $\mathcal{L}_X(H_1 + H_2) = \mathcal{L}_X H_1 + \mathcal{L}_X H_2$ [36], the Lie derivatives over $g_1, \ldots, g_4$ span all of $\mathcal{O}$.

The *observability codistribution* $d\mathcal{O}$ is defined as

$$d\mathcal{O}(q) = \text{span}\, dH(q) | H \in \mathcal{O}, q \in \mathcal{T} \tag{5}$$

By the *observability rank condition at* x^0, if $\dim \mathcal{T} = n$ and $\dim d\mathcal{O}(x^0) = n$, then the system is *locally weakly observable at* x^0.

To simplify the equations while calculating derivatives, we will take the measurement model to be an equivalent form,

$$o_{ji} = \frac{1}{2}(x_{ji}^2 + y_{ji}^2).$$

For reference, the Lie derivatives of a field h along a vector field f of orders 0 to n are defined as

$$\mathcal{L}_f^0 h = h \ , \qquad \mathcal{L}_f^1 h = \nabla h \cdot \mathbf{f} \ ,$$
$$\mathcal{L}_f^n h = \frac{\partial}{\partial T_{ji}}[\mathcal{L}_f^{n-1} h] \cdot \mathbf{f} \ .$$

From this we get

$$\begin{aligned}
\mathcal{L}^0 h &= \frac{1}{2}(x_{ji}^2 + y_{ji}^2) \\
\mathcal{L}_{g_1}^1 h &= -x_{ji} \\
\mathcal{L}_{g_2}^1 h &= 0 \\
\mathcal{L}_{g_3}^1 h &= x_{ji}\cos\theta_{ji} + y_{ji}\sin\theta_{ji} \\
\mathcal{L}_{g_4}^1 h &= 0
\end{aligned}$$

Therefore the space $d\mathcal{O}_0$ is spanned by

$$\nabla \mathcal{L}_h^0 = [x_{ji}, y_{ji}, 0]^T,$$

and the space $d\mathcal{O}_1$ is spanned by

$$\begin{aligned}
\nabla \mathcal{L}_{g_1}^1 &= [-1, 0, 0]^T \\
\nabla \mathcal{L}_{g_3}^1 &= [\cos\theta_{ji}, \sin\theta_{ji}, -x_{ji}\sin\theta_{ji} + y_{ji}\cos\theta_{ji}]^T.
\end{aligned}$$

From this we can see that the gradients of the Lie derivatives span the observation space. Interestingly, the values of measurements ω_i and ω_j do not affect the rank of the observation space. We can also determine that non-zero measurements of both v_i and v_j are required for the state to be fully observable, agreeing with the analysis in [6]. Therefore we can conclude that as long as both vehicles have non-zero linear velocity, it is possible to estimate their state using just a single range measurement, a fact that we verify experimentally in Sec V-A. We expect that in the $N > 2$ car case, the extra range measurements mean that fewer odometry measurements are necessary to observe the full state; however, such an analysis is outside the scope of this work.

D. EKF and UKF Formulation

We formulated the EKF and the UKF along standard lines, using the `FilterPy` Python package [37].

E. Particle Filter Formulation

We use a particle filter to estimate the posterior density $p(T_i^t | \boldsymbol{u}^0, \boldsymbol{o}^0, \ldots, \boldsymbol{u}^t, \boldsymbol{o}^t)$, where $\boldsymbol{u}^t$ and $\boldsymbol{o}^t$ represent odometry and range measurements from robot i or from any neighbor of robot i in any arbitrary order collected during time interval t. Note that the set of measurements over a given time period can be empty. Also note that the estimate of each transform is conditionally dependent on the other transforms due to the range measurements, and therefore the state of the system cannot be decomposed. Therefore the cars must share their range measurements, which we accomplish by using a wireless network, described in Sec. IV-B.

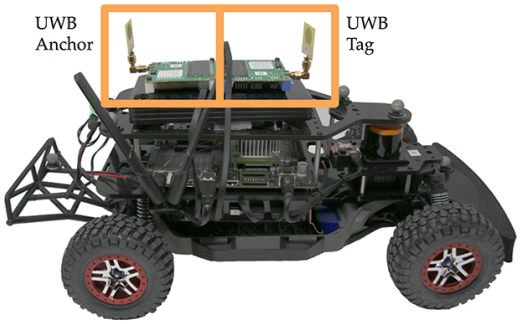

Fig. 3: Two Decawave ultra-wideband radios serve as the range sensors for our system.

We use a Sampling Importance Resampling (SIR) filter that uses systematic resampling. We allow for asynchronous update and predict steps that are determined by when we receive measurements from the sensors, and therefore time steps are non-constant. In fact, every measurement has a time stamp (the time stamps between robots are consistent due to the clock synchronization discussed in Sec. IV-C), and therefore we can calculate the dt between each measurement and the next; for any set of measurements received at time t, we define the array of time differences between consecutive measurements as $\boldsymbol{dt}^t$. The algorithm is described in detail in Alg. 1.

Algorithm 1 Asynchronous CL Particle Filter

Initialize M **particles** $T_{[1:M]}^1$ **and weights** $w_{[1:M]}^0$
Collect $\boldsymbol{u}^t \leftarrow$ odometry and $\boldsymbol{o}^t \leftarrow$ ranges
if $\boldsymbol{u}^t \neq \emptyset$ **then**
  for $k \leftarrow 1$ **to** M **do**
    Predict $T_{[k]}^t \leftarrow p(T_{[k]}^t | T_{[k]}^{t-1}, \boldsymbol{u}^t, \boldsymbol{dt}^t, \Sigma_u)$
  end for
end if
if $\boldsymbol{o}^t \neq \emptyset$ **then**
  for $k \leftarrow 1$ **to** M **do**
    Update $w_{[k]}^t \leftarrow w_{[k]}^{t-1}\, p(T_{[k]}^t | \boldsymbol{o}^t, \boldsymbol{dt}^t, \sigma_o)$
    Normalize $w_{[1:M]}^t \leftarrow w_{[1:M]}^t / \sum_{k=1}^M w_{[k]}^t$
    if $1/\sum_{k=1}^M (w_{[k]}^t)^2 < N_{eff}$ **then**
      Resample($T_{[1:M]}^t$, $w_{[1:M]}^t$)
    end if
  end for
end if
Compute $\mu_T \leftarrow \sum_{k=1}^M w_{[k]}^t T_{[k]}^t$
Compute $\Sigma_T^2 \leftarrow \sum_{k=1}^M w_{[k]}^t (T_{[k]}^t - \mu_T)(T_{[k]}^t - \mu_T)^T$
Return $\mu_T, \Sigma_T^2, T_{[1:M]}^t, w_{[1:M]}^t$

IV. Platform Overview

A. Hardware Platform

Our cars are based off of the MIT Racecar design [5]. The main components are a Traxxas Slash 4x4 chassis and an Nvidia Jetson TX2 on-board computer. Measurements are

collected from a Vedder electronic speed controller (ESC), which provides a speed estimate; a Traxxas 2075 servo, which controls the steering angle and from which angular velocity is derived; and two Decawave TREK1000 UWB evaluation modules. One Decawave sensor is configured to be an anchor, and one is configured to be a tag. The tags can only communicate with the anchors.

B. Communication

We use an open-source ROS multi-master system called Canopy [38]. The benefits of a multi-master system include:

- Selective message passing between ROS masters
- Vehicles can join and leave the server at will
- Communication through multiple networks

Although not tested in the following experiments, the use of a multi-master system to route messages over the internet would enable the cars to seamlessly exchange messages as they switch networks (for example as a car leaves an intersection and approaches another intersection); it would also allow the cars themselves to host the server so that no outside infrastructure would be necessary.

C. Clock Synchronization

Although UWBs can be used to do clock synchronization as well as ranging [24], we used the Network Time Protocol to synchronize the clocks on each vehicle. We did this so that our platform can work using other range sensors besides UWBs. We found that the clock error between vehicles using NTP was on average 2.0 ms with 8.9 ms standard deviation; this compares to an average delay of 84.0 ms with a standard deviation of 71.4 ms of packets sent across the network. Synchronized clocks allow us to use asynchronous filters. As the filters collect measurements from each car, each measurement comes with a time stamp. Because the filters receives messages at a rate faster than it can process (odometry information arrives at about 30 Hz from each car, and range measurements arrive at about 20 Hz, meaning that the particle filter receives around 250 measurements per second for the five-car case), they collect odometry messages for a short period of time (about 30 ms), then use the time stamp of the most recent message as the approximate time stamp for all of the messages they have collected. They store the time stamp from the previous batch so that they can calculate the time step between the two batches. Since range measurements arrive at a slightly slower rate and are faster to process (unlike for the odometry measurements, we do not have to propagate the dynamics using Runge-Kutta), we run a predict step every time we receive a range measurement.

V. Experimental Evaluation

Our experiments were performed under realistic conditions, with packet loss, communication delays, and non-constant velocities, along with the usual measurement and process noise. Moreover, the model cars have dynamics that are similar to the dynamics of real cars because they have a suspension system and Ackermann steering. Therefore, our experimental setup includes many of the adversarial conditions that one would expect to encounter in the real world.

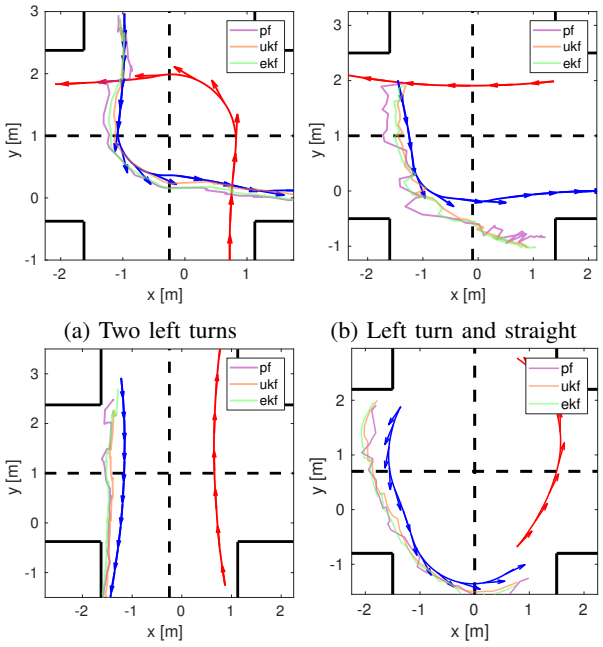

(a) Two left turns (b) Left turn and straight

(c) Both straight (d) Semicircles

Fig. 4: Two Car Experiments. Ground-truth car trajectories (blue and red) for our two car experiments and the resulting estimates (light lines) of the blue car's position from the frame of the red car.

We collected datasets of scenarios involving two and five cars; all of the adversarial conditions encountered during the recording are preserved in the recorded dataset. Odometry data is received from each car at a rate of about 30 Hz, and range measurements arrive at a rate of 10-20 Hz from each car. Ground-truth was collected using a Vicon motion capture system.

A. Two Car Experiments

RMSE	Filter	Left Turns	Left Turn/ Straight	Straight	Semicircle
Dist [m]	PF	0.26	**0.41**	0.32	0.33
	UKF	0.26	0.80	**0.29**	**0.29**
	EKF	**0.25**	0.85	0.33	0.33
Theta [m]	PF	0.11	**0.17**	0.08	0.15
	UKF	0.10	0.27	0.03	**0.03**
	EKF	**0.09**	0.28	**0.02**	0.08

TABLE I: RMSE distance and bearing error for the two car tests.

We ran four different two-car experiments to test the accuracy of localization using just a single range measurement (as well as odometry measurements). We tested four different scenarios, shown in Fig. 4. The first three scenarios, "two left turns", "left turn and straight", and "both straight", are scenarios often encountered at intersections.

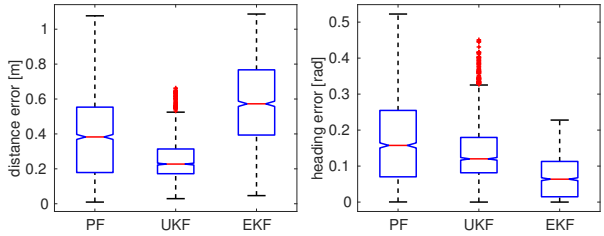

(a) Distance error (b) Heading error

Fig. 5: Five Car Experiment. Boxplots of the errors in distance and heading for each filter.

The last scenario, "semicircles", occurs at rings such as roundabouts. In the figures, the red line is the ground-truth trajectory of the egocar; the dark blue line is the ground-truth trajectory of the other car; and the light lines are the egocar's estimates of the other car using a particle filter, a UKF, and an EKF. The results of the experiments are recorded in Table I. Interestingly, no single filter clearly outperforms the others. The EKF and UKF do very poorly on the "left turn and straight" experiment; however, they perform about the same or better than the particle filter in the other tests. The RMSE of the distances are in the range of 25-81 cm, which is comparable to other work using real-world data [39], [10], [40], [32]. However, unlike other work, this result was achieved using just one range measurement between two moving platforms.

B. Five Car Experiment

We ran one test with five cars in an intersection scenario; the cars are shown in Fig. 1, and their trajectories (along with the trajectories estimated by the UKF) are shown in Fig. 6. Four of the cars made left turns, while one car traveled straight across the intersection. Since we found it to be nearly impossible for the five cars to navigate the intersection simultaneously, we had the cars move in three separate groups. First, the red (ego) and green cars made left turns. Second, the pink car drove straight across the intersection. Finally, the orange and blue cars made left turns. As can be seen in Table II, the UKF outperforms the other filters in estimating the relative transforms. The distribution of errors for the filters can be seen more clearly in Fig. 5. The UKF achieves the lowest distance error, while the EKF achieves the lowest heading error.

RMSE	Filter	T_{21}	T_{31}	T_{41}	T_{51}
Dist [m]	PF	0.31	0.43	0.26	0.44
	UKF	**0.26**	**0.20**	**0.29**	**0.32**
	EKF	0.36	0.80	0.64	0.59
Theta [rad]	PF	0.22	0.20	0.24	0.38
	UKF	0.20	**0.18**	**0.17**	**0.16**
	EKF	**0.14**	**0.18**	0.29	0.34

TABLE II: Five Car Experiment. RMSE distance and heading error

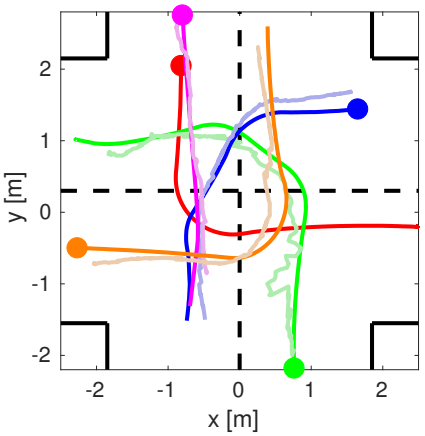

Fig. 6: Five Car Experiment, showing UKF estimates. Ground-truth trajectories are the darker lines. The estimates, as computed from and relative to the red car are shown in lighter colors. The starting positions are denoted by the circles.

VI. Discussion and Conclusion

In this work, we considered cooperative localization based on range measurements. We presented a new reformulation of the relative transform between two unicycle models, and we performed a nonlinear observability analysis that showed that the linear velocities of the system must be non-zero in order to achieve full observability. We incorporated our model into an asynchronous particle filter, UKF, and EKF that consider odometry and range information. We also designed an experimenetal system that uses UWB radios, a ROS multimaster system, and high performance RC cars to approximate real-world driving scenarios. We evaluated our framework on experiments involving two and five cars. Our experimental results show that, despite the nonlinearity of the measurement model, the UKF and EKF typically achieve better results than the particle filter. In addition, the UKF and EKF require much less computation than the particle filter. Since the UKF outperforms the EKF, we find that the UKF is the best filter for the task of estimating relative transforms between cars using range measurements.

Acknowledgments

The present work has received funding from Toyota Research Institute within the Toyota-CSAIL joint research center and Office of Naval Research grant ONR N000141812830. The views expressed in this paper solely reflect the opinions and conclusions of its authors and not the funding agencies.

References

[1] W. Schwarting, J. Alonso-Mora, and D. Rus, "Planning and decision-making for autonomous vehicles," *Annual Review of Control, Robotics, and Autonomous Systems*, vol. 1, pp. 187–210, 2018.

[2] S. Fujii, A. Fujita, T. Umedu, S. Kaneda, H. Yamaguchi, T. Higashino, and M. Takai, "Cooperative vehicle positioning via v2v communications and onboard sensors," in *2011 IEEE Vehicular Technology Conference (VTC Fall)*. IEEE, 2011, pp. 1–5.

[3] K. Witrisal, P. Meissner, E. Leitinger, Y. Shen, C. Gustafson, F. Tufvesson, K. Haneda, D. Dardari, A. F. Molisch, A. Conti, *et al.*, "High-accuracy localization for assisted living: 5g systems will turn multipath channels from foe to friend," *IEEE Signal Processing Magazine*, vol. 33, no. 2, pp. 59–70, 2016.

[4] G.-M. Hoang, B. Denis, J. Härri, and D. T. Slock, "Cooperative localization in gnss-aided vanets with accurate ir-uwb range measurements," in *2016 13th Workshop on Positioning, Navigation and Communications (WPNC)*. IEEE, 2016, pp. 1–6.

[5] "MIT RACECAR," https://mit-racecar.github.io/.

[6] A. Martinelli and R. Siegwart, "Observability Analysis for Mobile Robot Localization," in *Proceedings of the International Conference on Intelligent Robots and Systems (IROS)*, 2005.

[7] K. Leung, Y. Halpern, T. Barfoot, and H. Liu, "The UTIAS Multi-Robot Cooperative Localization and mapping dataset," *The International Journal of Robotics Research*, vol. 30, no. 8, 2011.

[8] A. K. Das, R. Fierro, V. Kumar, J. P. Ostrowski, J. Spletzer, and C. J. Taylor, "A Vision-based Formation Control Framework," *IEEE Transactions on Robotics and Automation*, vol. 18, no. 5, 2002.

[9] A. Mourikis and S. Roumeliotis, "Performance Analysis of Multirobot Cooperative Localization," *IEEE Transactions on Robotics*, vol. 22, no. 4, 2006.

[10] T.-K. Chang, S. Chen, and A. Mehta, "Multirobot Cooperative Localization Algorithm with Explicit Communication and its Topology Analysis," in *Proceedings of the International Symposium on Robotics Research (ISRR)*, 2017.

[11] F. Meyer, O. Hlinka, H. Wymeersch, E. Riegler, and F. Hlawatsch, "Distributed Localization and Tracking of Mobile Networks Including Noncooperative Objects," *Transactions on Signal and Information Processing over Networks*, vol. 2, no. 1, 2016.

[12] "Decawave," http://www.decawave.com/, 2017, accessed: 2018-09-15.

[13] T. Schneider, M. Dymczyk, M. Fehr, K. Egger, S. Lynen, I. Gilitschenski, and R. Siegwart, "Maplab: An Open Framework for Research in Visual-Inertial Mapping and Localization," *Robotics and Automation Letters*, vol. 3, no. 3, 2018.

[14] W. Churchill and P. Newman, "Experience-based Navigation for Long-Term Localisation," *The International Journal of Robotics Research*, vol. 32, no. 14, 2013.

[15] T. Cieslewski, S. Lynen, M. Dymczyk, S. Magnenat, and R. Siegwart, "Map API - Scalable Decentralized Map Building for Robots," in *Proceedings of the IEEE International Conference on Robotics and Automation (ICRA)*, 2015.

[16] M. Gadd and P. Newman, "Checkout My Map: Version Control for Fleetwide Visual Localisation," in *Proceedings of the International Conference on Intelligent Robots and Systems (IROS)*, 2016.

[17] A. Cunningham, M. Paluri, and F. Dellaert, "DDF-SAM: Fully distributed SLAM using Constrained Factor Graphs," in *Proceedings of the IEEE/RSJ International Conference on Intelligent Robots and Systems (IROS)*, 2010.

[18] A. Martinelli, F. Pont, and R. Siegwart, "Multi-robot Localization Using Relative Observations," in *Proceedings of the International Conference on Robotics and Automation (ICRA)*, 2005.

[19] L. Luft, T. Schubert, S. Roumeliotis, and W. Burgard, "Recursive Decentralized Collaborative Localization for Sparsely Communicating Robots," in *Proceedings of Robotics: Science and Systems (RSS)*, 2016.

[20] S. Panzieri, F. Pascucci, and R. Setola, "Multirobot Localisation Using Interlaced Extended Kalman Filter," in *Proceedings of the IEEE/RSJ International Conference on Intelligent Robots and Systems (IROS)*, 2006.

[21] N. Karam, F. Chausse, R. Aufrere, and R. Chapuis, "Localization of a Group of Communicating Vehicles by State Exchange," in *Proceedings of the IEEE/RSJ International Conference on Intelligent Robots and Systems (IROS)*, 2006.

[22] H. Li, F. Nashashibi, and M. Yang, "Split Covariance Intersection Filter: Theory and Its Application to Vehicle Localization," *IEEE Transactions on Intelligent Transportation Systems*, vol. 14, no. 4, 2013.

[23] Q. Sun, M. Diao, Y. Zhang, and Y. Li, "Cooperative localization algorithm for multiple mobile robot system in indoor environment based on variance component estimation," *Symmetry*, vol. 9, no. 6, p. 94, 2017.

[24] F. Meyer, B. Etzlinger, F. Hlawatsch, and A. Springer, "A Distributed Particle-based Belief Propagation Algorithm for Cooperative Simultaneous Localization and Synchronization," in *Proceedings of the Conference on Signals, Systems and Computers*, 2013.

[25] R. Olfati-Saber, "Distributed Kalman Filter with Embedded Consensus Filters," in *Proceedings of the Conference on Decision and Control (CDC)*, 2005.

[26] S. Julier and J. Uhlmann, "A Non-Divergent Estimation Algorithm in the Presence of Unknown Correlations," in *Proceedings of the American Control Conference (ACC)*, 1997.

[27] S. Cedervall and X. Hu, "Nonlinear observers for unicycle robots with range sensors," *IEEE transactions on automatic control*, vol. 52, no. 7, 2007.

[28] R. Sharma, R. W. Beard, C. N. Taylor, and S. Quebe, "Graph-based observability analysis of bearing-only cooperative localization," *Transactions on Robotics*, vol. 28, no. 2, 2012.

[29] G. Papadopoulos, M. F. Fallon, J. J. Leonard, and N. M. Patrikalakis, "Cooperative Localization of Marine Vehicles using Nonlinear State Estimation," in *Proceedings of the International Conference on Intelligent Robots and Systems (IROS)*, 2010.

[30] A. Wallar, B. Araki, R. Chang, J. Alonso-Mora, and D. Rus, "Foresight: Remote Sensing for Autonomous Vehicles Using a Small Unmanned Aerial Vehicle," in *Proceedings of the Conference on Field and Service Robotics (FSR)*, 2017.

[31] B. Hepp, T. Nageli, and O. Hilliges, "Omni-directional Person Tracking on a Flying Robot Using Occlusion-robust ultra-wideband signals," in *Proceedings of the International Conference on Intelligent Robots and Systems (IROS)*, 2016.

[32] K. Guo, Z. Qiu, W. Meng, L. Xie, and R. Teo, "Ultra-wideband based Cooperative Relative Localization Algorithm and Experiments for Multiple Unmanned Aerial Vehicles in GPS Denied Environments," *International Journal of Micro Air Vehicles*, vol. 9, no. 3, 2017.

[33] A. Bahr, J. Leonard, and M. Fallon, "Cooperative Localization for Autonomous Underwater Vehicles," *The International Journal of Robotics Research*, vol. 28, no. 6, 2009.

[34] A. Bahr, M. Walter, and J. Leonard, "Consistent Cooperative Localization," in *Proceedings of the International Conference on Robotics and Automation (ICRA)*, 2009.

[35] R. Hermann and A. Krener, "Nonlinear Controllability and Observability," *Transactions on Automatic Control*, vol. 22, no. 5, 1977.

[36] H. Nijmeijer and A. van der Schaft, "Controllability and observability, local decompositions," in *Nonlinear Dynamical Control Systems*, 1990.

[37] R. Labbe, "Kalman and bayesian filters in python," https://github.com/rlabbe/Kalman-and-Bayesian-Filters-in-Python, 2018.

[38] A. Wallar, "Canopy," https://github.com/canopy-ros, 2017.

[39] B. Teague, Z. Liu, F. Meyer, and M. Z. Win, "Peregrine: 3-d network localization and navigation," in *Communications (LATINCOM), 2017 IEEE 9th Latin-American Conference on*. IEEE, 2017.

[40] A. Howard, M. J. Mataric, and G. S. Sukhatme, "Putting the'i'in'team': An ego-centric approach to cooperative localization," in *Robotics and Automation, 2003. Proceedings. ICRA'03. IEEE International Conference on*, vol. 1. IEEE, 2003.